*Article*

# Thermal and Energy-Efficiency Assessment of Novel Hybrid CLT-Glass Facade Elements

**Vlatka Rajčić [1,*], Nikola Perković [2], Chiara Bedon[3], Jure Barbalić[4], Roko Žarnić[5]**

[1] University of Zagreb, Croatia, vrajcic@grad.hr
[2] University of Zagreb, Croatia, nperkovic@grad.hr
[3] University of Trieste, Italy, chiara.bedon@dia.units.it
[4] University of Zagreb, Croatia, jbarbalic@grad.hr
[5] University of Ljubljana, Slovenia, roko.zarnic@fgg.uni-lj.si
* Correspondence: vrajcic@grad.hr;

**Abstract:** Facade elements are known to represent a building component with multiple performance parameters to satisfy. Among others, "advanced facades" take advantage of hybrid solutions, like the assemblage of laminated materials. In addition to enhanced mechanical properties that are typical of optimally composed hybrid structural components, these systems are energy-efficient, durable, and offer lightening comfort and optimal thermal performance. This is the case of the structural solution developed in joint research efforts of the University of Zagreb and the University of Ljubljana, within the Croatian Science Foundation VETROLIGNUM project. The design concept involves the mechanical interaction of timber and glass load-bearing members, without sealing or bonded glass-to-timber surfaces. Laminated glass infilled timber frames are recognized as a new generation of structural members with relevant load-carrying capacity (and especially the enhancement of earthquake resistance of framed systems), but also energy-efficient and cost-effective solutions. In this paper, a special focus is then dedicated to the thermal performance assessment of these innovative CLT-glass facade modules under ordinary operational conditions. Numerical modelling of a full-scale mock-up building is first presented, by taking advantage of continuous ambient records of environmental and thermal comfort parameters. Afterward, a more detailed Finite Element (FE) numerical analysis is carried out at the component level (CLT-glass facade element). The numerical results show that the even the use of a bare / thermally no optimized CLT-glass composite panel for facade systems can be energy efficient and offer stable thermal performances, that are almost in line with national and European standards requirements.

**Keywords:** Cross-Laminated Timber (CLT), laminated glass, hybrid facade element, thermal performance, energy efficiency, numerical modelling

## 1. Introduction

In the last decade, there has been a progressive development of load-bearing building components composed of timber and glass, firstly beams [1- 4]. Later, even more attention has been dedicated to curtain wall applications, where wide surfaces must be covered and enhanced load-bearing performances/deformation capacities must be satisfied, especially under extreme design loads such as earthquakes [5, 6]. In most of the cases, however, the explored solutions and design applications still involve a continuous (adhesive and/or mechanical) connection between a given timber frame and the glass infill panels (Figure 1).

Preprints (www.preprints.org) | NOT PEER-REVIEWED | Posted: 23 March 2020 doi:10.20944/preprints202003.0330.v1

Peer-reviewed version available at Appl. Sci. 2020, 10, 3071; doi:10.3390/app10093071



Besides the need for optimal structural performances for these innovative solutions, moreover, a facade element as a whole should fulfill a multitude of performance requirements, including the thermal response, energy efficiency, waterproofness, airtightness, etc.

(a) (b)

**Figure 1.** Examples of timber-glass facade solutions: (a) typical cross-section of curtain wall detail (www.stabalux.com); (b) adhesively bonded framed panels according to [5].

One successful solution is a hybrid multi-purpose panel composed of a CLT frame and two double sheets of laminated glass, where wood and glass contact is achieved only through friction interactions. The panel was developed inside the VETROLIGNUM project (www.grad.unizg.hr/vetrolignum). A series of tests whose results are published in [7-9] have demonstrated good load-bearing capacity for static and dynamic loads, good stability, serviceability, earthquake resistance and excellent ability to dissipate seismic energy by friction and ductile behaviour of connector in the corner of the CLT frame.

As could be seen in Figure 2, panels were made of CLT frames (with the cross-section dimension b/h = 90/160 mm). Laminated glass sheets are installed in the frame without sealant along with the glass-to-timber contact. The glass infill was made of two-ply, laminated semi-tempered layers bonded by Ethylene Vinyl Acetate (EVA®) foils. The thickness of each glass sheet was set in 10mm, while the thickness of the Bridgestone EVASAFE adhesive bond was 1.6mm. A continuous, flexible rubber edge trim (Figure 2b) was used to seal the interposed air cavity, with its thickness s= 12.8mm. The edges of the tested glass sheets were trapezoidal polished, to remove all those micro-cracks and potential weak regions where glass damage could initiate during the mechanical loading stage.

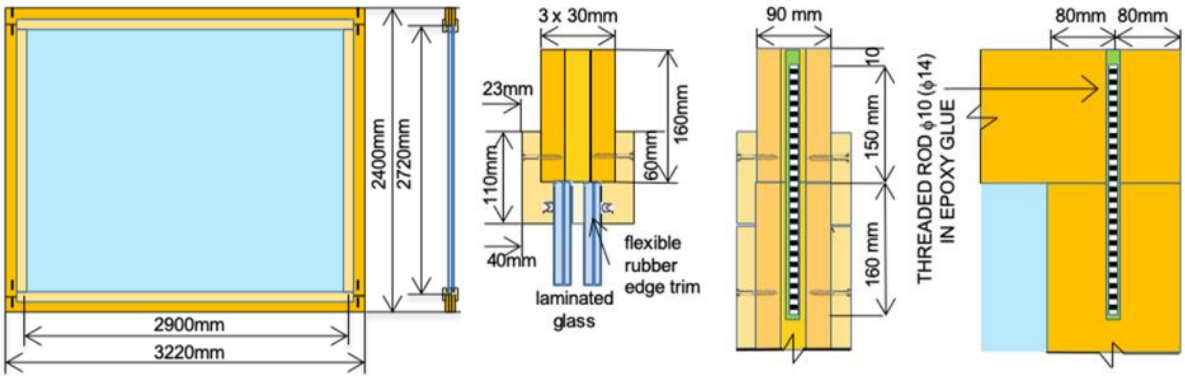


(a) (b) (c)

**Figure 2.** Full-scale CLT-glass facade element: (a) front view, (b) CLT-to-glass frame connection detail (cross-section) and (c) timber frame corner joint.

The VETROLIGNUM system takes the best characteristics of two breaking and rather new building materials, Cross-Laminated Timber and laminated glass, by optimizing the interaction between them. It is daily recognized that wooden buildings whether designing for the light frame or mass timber structural systems (panel or frame systems, etc.), can benefit from the material's versatility, benefits to occupants, as well as thermal, acoustic, seismic and fire performances. CLT is a relatively new structural engineered wood panel system that is gaining popularity all over the world. Typical applications for CLT in buildings include floors, walls, and roofing. The panels' ability to resist high racking and compressive forces makes them especially cost-effective for multi-storey and long-span diaphragm applications. CLT is the basis of tall wood movements, as the material's high strength, dimensional stability and rigidity allow it to be used in mid- and high-rise construction [10]. Additionally, it has favourable aesthetic, energy and environmental, properties that enhance its intrinsic qualities [11]. Also, structural glass has recently been more widely used as the structural material for transfer various types of loads and being used under different boundary conditions. Glass products are well covered by European norms. [12, 13], Harmonised European norms for the comprehensive structural design of load-bearing glass elements are in preparation and should be presented to designers in 2021 [14-16]. Meanwhile, there are many national documents (technical regulations or technical guidelines) for verification of glass elements (see for example [17-19]). However, there are still several open questions regarding the design of load-bearing glass. Among others, one of the challenging issues that will be partly addressed in this paper is related to the increased thermal exposure of glass in facades, and its effects on the mechanical properties of load-bearing glass systems [20-23].

## 2. Thermal and energy efficiency assessment of facade components

Testing the energy performance assessment of innovative load-bearing solutions and components for buildings represents a crucial step in research and design. The facade enclosure is, in fact, a key factor in defining the energy rating and class of the entire building it belongs to, as well as the thermal comfort of occupants. Accordingly, it must satisfy specific performance limits [25].
Such an issue represents a strategic design step for the assessment and optimization of novel envelope systems, and literature studies can be found for different structural solutions [26-29].
In some cases, timber components have been explored in the form of cladding elements for facades [30]. Even more advanced calculation methods are then required in the case of innovative facade solutions, such as "adaptive" systems [31].

### *2.1. Reference thermal performance indicators*

Following the EN ISO 13788 standard [32], among others, one of the performance parameters to assess is the thermal quality, which can be generally expressed by the well-known temperature factor at the internal surface $f_{Rsi}$. The simplified calculation approach presented in [32] suggests that:

$$f_{Rsi} = \frac{T_{si} - T_{out}}{T_{int} - T_{out}} \quad (1)$$

with $T_{si,}$ the temperatures of the internal wall surface, $T_{int}$ the internal air temperature and $T_{out}$ external air temperature respectively. The internal surface temperature strictly depends on the features of the structure to investigate and can be sensitive especially to thermal bridges causing multidimensional heat flow. Another relevant parameter is represented by the internal surface resistance, which depends on convection and radiation coefficients, on the air movements in the room, on the air and surface temperature distribution in the room and on the surface material properties. Accordingly, refined and time-consuming numerical models of a given room as a whole would be necessarily required, to account for several aspects like the thermal resistances of the surrounding envelopes, the environmental temperature, the air distribution in the room and its

geometry. However, simplified calculation methods or input values recommended by existing guideline documents can be used for preliminary estimates.

The temperature factor $f_{Rsi}$ should be generally close to the unit to represent optimally insulated buildings. In any case, to ensure the occurrence of mould growth and surface condensation in dwellings, $f_{Rsi}$ is generally accepted for values at least equal to $f_{Rsi} \geq 0.75$. Besides the general calculation approach in the EN ISO 13788 provisions, moreover, a series of National guidelines are available in several countries to recommend minimum limit values for $f_{Rsi}$. These are range of $f_{Rsi} \geq 0.52$ (France), or $f_{Rsi} \geq 0.65$ (Netherlands) and $f_{Rsi} \geq 0.7$ for Germany [33].

With the outside climate (temperature and relative humidity), four main parameters control the surface condensation and development of fungi, namely:

- the "thermal quality" of peripheral elements of a building is represented by thermal resistance, thermal bridges, geometry and internal surface resistance; this is defined by the temperature factor on the inner surface, $f_{Rsi}$;
- the internal humidity, influencing the dew point in the air;
- indoor air temperature: lower room temperature is generally more critical especially for rooms with reduced, intermittent heating, or in unheated rooms where water vapour can escape from adjacent heated rooms;
- heating systems, that affects air movement and temperature distribution

Many problems can occur and the main ones are:

a) molds that occur when the surface humidity is more than 80% over several days,
b) the danger of material corrosion: it should be checked for each building part of a heated building that the $f_{Rsi}$ on the interior surface is less than the maximum permissible factor for critical surface humidity,
c) too low surface temperature (contact exterior surfaces of heated spaces, caused by poor external thermal insulation of the building part, thermal bridges, an arrangement of furniture),
d) increase in humidity caused by an increase in air humidity above the design values at the position of contact of the air with the wall (caused by inappropriate use of space, airflow).

### *2.2. Climate changes and design challenges for facades*

As known, climate changes over time. Climate variability can be caused by natural factors within the climate system itself. The natural variability of the climate can also be caused by external factors, such as the large number of aerosols ejected by a volcanic eruption into the atmosphere or the change in solar radiation that reaches the atmosphere and the Earth's surface. In addition to these natural variations of climate, climate change caused by human activities (anthropogenic impact on climate), which emit greenhouse gases into the atmosphere, are of great interest, and they play a key role in warming the atmosphere.

Besides the envelope features, however, the reference $f_{Rsi}$ minimum value is related to climate conditions and climate changes. Accordingly, new building envelopes and systems should be able to properly satisfy a set of thermal performance requisites that become even more restrictive as far as the climate conditions modify. Following a past Köppen's classification for the Croatian region (see [34] and Figure 3a), for example, the largest National part was detected to have a moderately warm rainy climate, with mean monthly temperature in the coldest month of the year above -3°C and below 18°C. The highest mountain regions only (with > 1200m of altitude) were recognized to have a snowy, forest climate, with the mean temperature in the coldest month below -3 °C. In the continental mainland, finally, the hottest month of the year was usually detected in a mean temperature lower (and in the coastal area higher) than 22 °C.

Such a literature study, as in most other cases, actually underestimates the real climate conditions of

several regions. Within the VETROLIGNUM project, field ambient measurements have been recorded over a period of 3 years, giving evidence of typical temperature records according to Figure 3b.

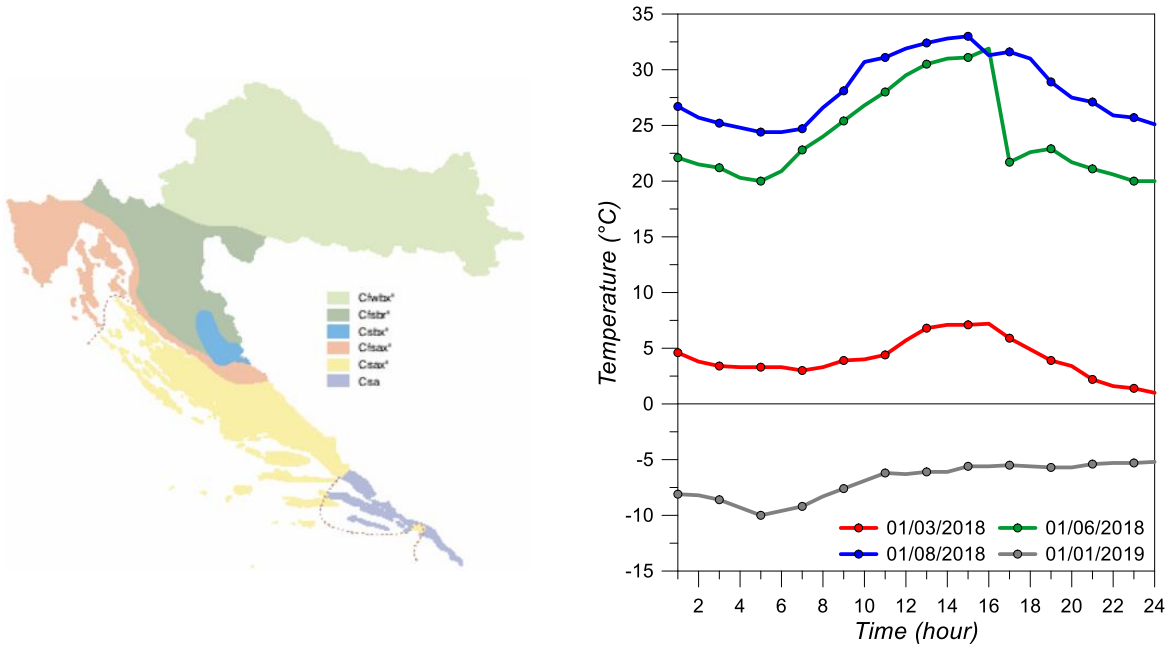


*(a)* *(b)*

**Figure 3.** Ambient conditions: (a) Köppen's classification (2003 proposal) for the Croatian climate (reproduced from [34]), and (b) meteorological data (selection) from the VETROLIGNIUM framework (University of Zagreb).

## 3 Mock-up building and experimental investigation

### *3.1. Live-Lab mock-up building*

Given the design challenges and requirements summarized in Section 2, this paper experimentally and numerically explores the thermal performance and energy efficiency of a full-scale CLT-glass building prototype that has been proposed in the framework of the VETROLIGNUM project.
For the purpose of testing the thermal and physical characteristics of the CLT-glass hybrid system, the mock-up building, herein called the "Live-Lab" facility, was constructed in 2018.
The facility, Figure 4, actually consists of a full-size, single space characterized by plan dimensions B=3.22m × W=2.80m, with H= 2.8m the height. The 3D building is located on the roof of a single story building not accessible to the public, at the University of Zagreb, Faculty of Civil Engineering. The main transversal facades of the mock-up building consist of full-size CLT-glass modules for the East and West envelopes.
The mock-up is constructed in a way that enables (i.e., for re-use in future mock-up configurations) the removal of the CLT-glass facade elements, and the introduction of solid timber walls (detail of Figure 4).

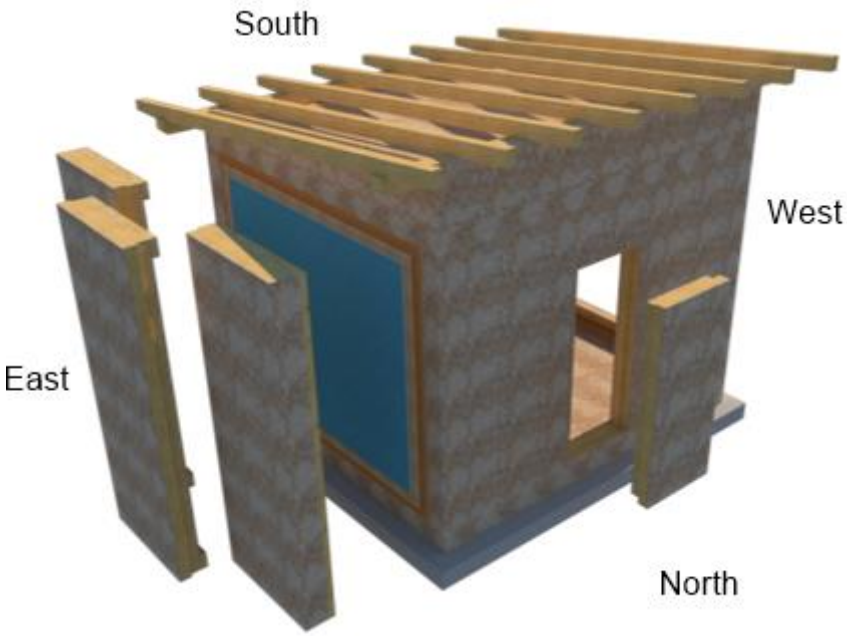


*(a)*

*(b)*

*(c)*

**Figure 4.** Assembly process for the Live-Lab facility at the University of Zagreb (2018): (a) general concept; (b) CLT-glass facade elements and (c) roof installation.

The geometry and detailing of the other building components (longitudinal walls, floor, and roof), accordingly, were defined based on the expected load-bearing capacity (preliminary static calculations under ordinary loads) and energy requirements. Prefabricated panels of typical use for the construction of wooden houses were used, to obtain a lightweight framework system inclusive of Oriented Strand Boards (OSB) panels and thermal insulation layers. The South longitudinal wall was obtained by a full-scale single panel. On the opposite side, the North wall was composed of two partitions, to possibly account for the presence of a door (Figure 4a). Two adjacent panels, mechanically interconnected, were used to realize the floor. The single-pitch roof consists of ceiling supporting attic panels, and roof beams.

### *3.2. Material properties*

All the panels are composed of KVH solid structural timber marked by class C24 (spruce) according to EN 338 provisions [35], dried up to 18% of humidity. The timber members are positioned in the

form of frames with lintels and studs, the geometry is determined based on a static calculation. Between the timber frame members, an insulation material is used (multi-purpose NaturBoard VENTI mineral wool boards, 600 × 1000mm (200mm thick), by KNAUF Insulation [36]). A Delta-Dawi GP steam barrier is also installed inside the panel (above the insulation), and sealed with appropriate straps [37].

On both sides, the timber frames are finally lined with OSB elements (125 × 2500mm their size, 18 mm in thickness) with an impregnating finisher, to ensure water resistance. All the joints are made of zinc-plated bolts or nails, whose detailing is based on preliminary static calculations.

## 4. The testing program for the CLT-glass facade performance assessment

The experimental measurements for the 3D building prototype of Figure 4 were conducted in a one-year cycle, hereinafter referred to as "Cycle 1" (September 2018 - August 2019). The latter, in the framework of the ongoing VETROLIGNUM project, will be followed by further field measurements.

The so-called Cycle 1 included:

- indoor Relative Humidity (RH) and temperature,
- outdoor RH and temperature,
- RH + temperature data within the cavity of double insulated glass, and
- preliminary measurements of the energy consumption of the 3D building system.

In parallel to ambient measurements, a thermographic camera was used to capture possible relevant thermal bridges, as well as critical details of the Live-Lab assembly, with careful consideration for the region of joints and corners.

### *4.1. Instruments*

The external climate parameters (wind speed, wind direction, precipitations, temperature, and humidity) in the Live-Lab context were measured by means of a meteorological station (Figure 5).

The latter was combined with a central control station designed by SITEL d.o.o. (Ljubljana, Slovenia (www.sitel.si)), to support the continuous monitoring of climate conditions and the acquisition of relevant data.

As a particularity of the Live-Lab facility, a heating source was also taken into account for the cavity between two glass panels. As the hygrothermal properties in the cavity were set as a control parameter for the continuous measurement, the heater was set to automatically switch on at the first attainment of the dew point for glass.

In the post-processing stage, based on the collected measurement data, the impact of such a kind of heating source was assessed in terms of the sensitivity of the thermal transmission of the 3D facility as a whole. The latter was also assessed in terms of impact on the energy consumption for maintaining a constant indoor temperature for the facility. To optimize the energy consumption of the Live-Lab prototype, solar panels were installed on the roof, to act as an additional external energy source. Electricity for heating or cooling of the facility was thus supplied both from the electricity grid and from the solar panels.

Setup instruments, finally, included an air conditioner and a fan, to reproduce the typical configuration of residential and commercial buildings.

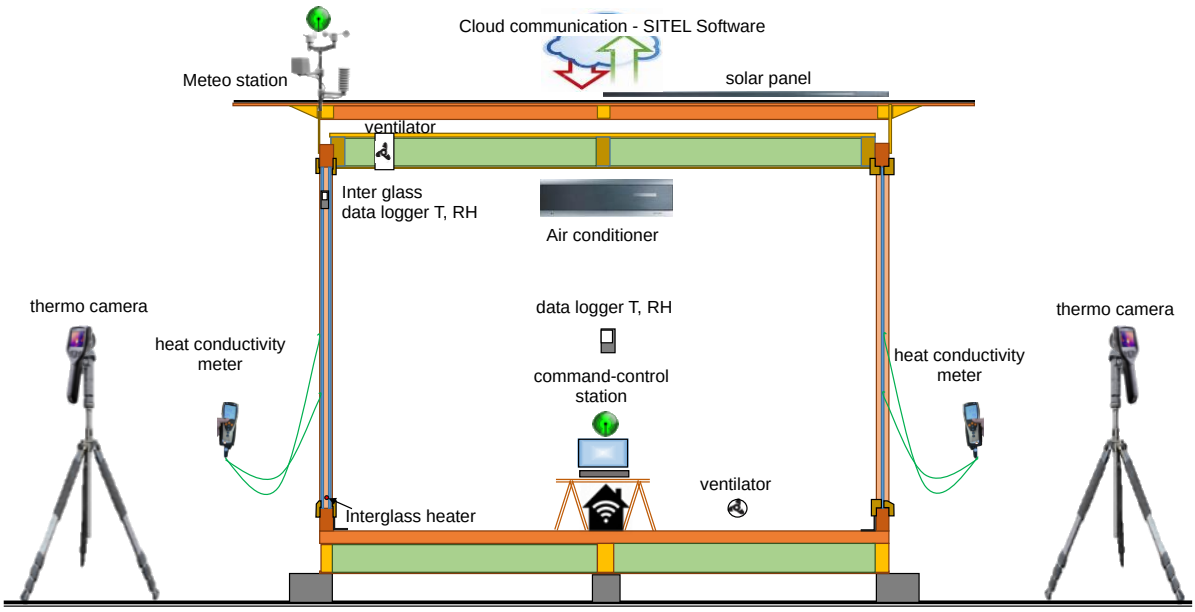


**Figure 5.** Instruments for the field experimental measurements (schematic cross-section of the Live-Lab mock-up building).

### *4.2. Experimental results*

In Figure 7, major outcomes from continuous indoor monitoring of the Live-Lab facility are proposed in terms of temperature and RH records. Depending on the external climate conditions (Figure 4b), major efforts were spent to achieve comfortable hygrothermal conditions inside the building, in line with conventional human habitation parameters.

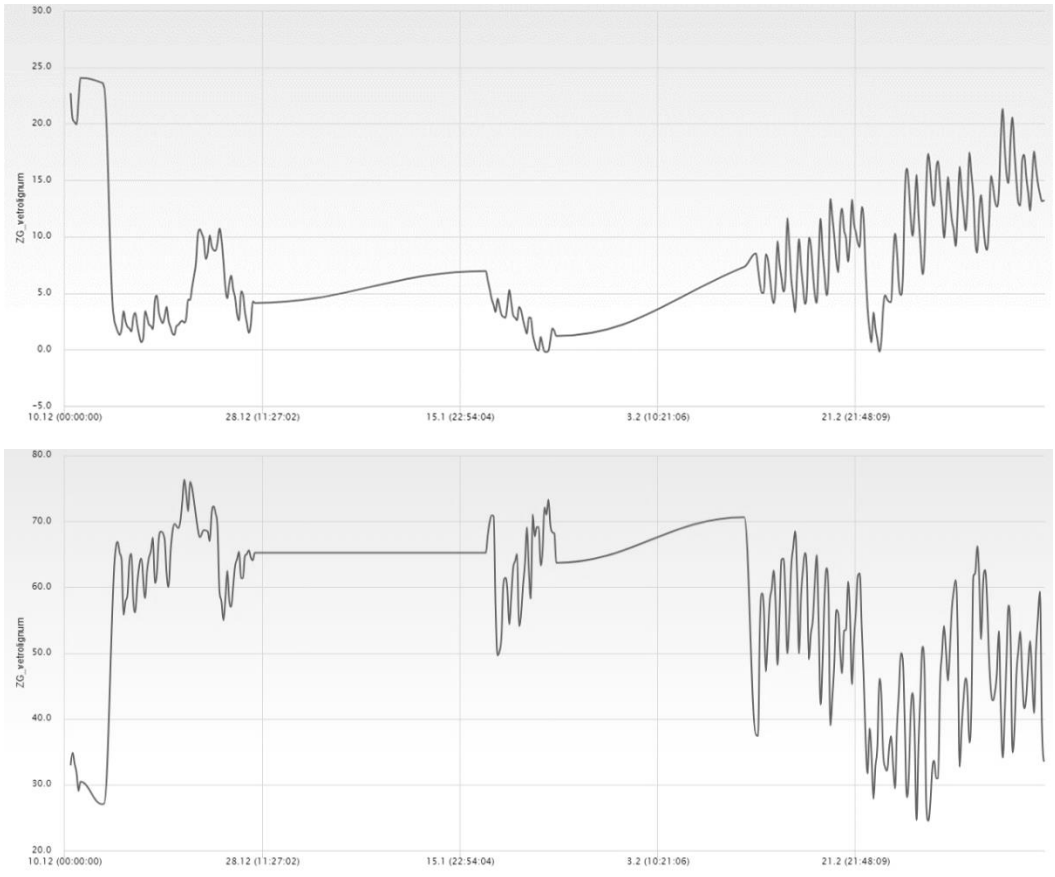


*(a)*

*(b)*

**Figure 6.** Live-Lab indoor measurements from SITEL control station: (a) temperature and (b) relative humidity.

Careful consideration was spent also for the monitoring of hygrothermal conditions in the glass cavity, where the heater source was installed.

During continuous monitoring, slightly higher energy consumption was observed to reach the required indoor conditions. The reason was found in the presence of linear thermal bridges that were properly detected in the critical details with the support of thermal cameras. As expected, see Figure 8, major temperature scatter and variations were found especially in the region of transition from timber to glass.

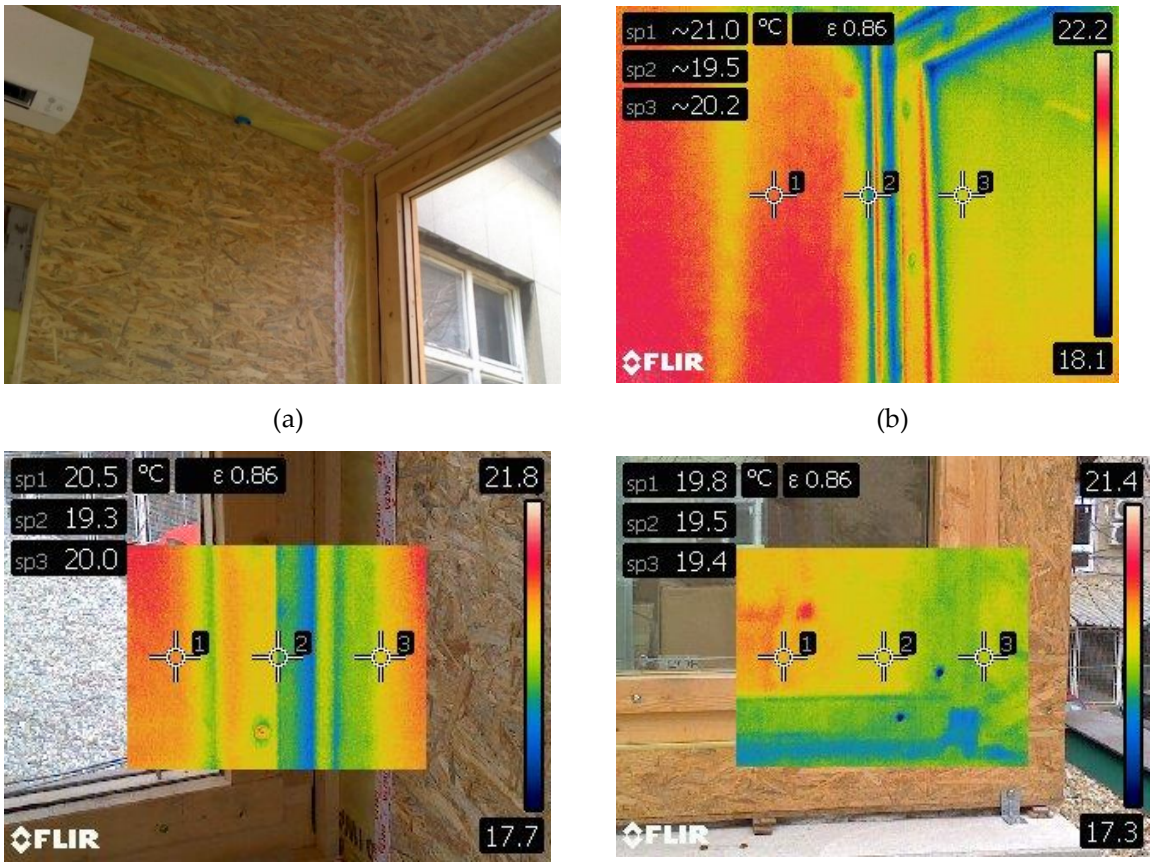


(a) (b)

(c) (d)

**Figure 7.** Thermal bridges detected by thermal camera acquisitions: (a) top corner layout (indoor), with (b) corresponding temperature field, and (c)-(d) bottom corner detail (indoor and outdoor measurements).

## 5. Full-size numerical analysis of the Live-Lab facility

Numerical simulations, as known, represent one of the most powerful tools in support of design optimization and assessment. The basic concept that it is reasonably cost/time conservative to develop a virtual model (based on well-known physical processes and constitutive laws) rather than a real experimental prototype. This applies especially to full-size building assemblies and complex systems, like the Live-Lab 3D facility investigated in this paper. More in detail, a series of numerical simulations were carried out with the EnCert-HR computer software (*www.encert.hr*), to calculate – as much accurately as possible – the expected thermal loads (i.e., thermal losses and gains) and the overall energy consumption (thus the energy efficiency) of the 3D building facility. In doing so, the reference modelling procedure proposed in Figure 8 was taken into account. All the calculation

process was developed by accounting for the nominal geometrical and thermo-physical properties of materials in use, as well as the available meteorological data from continuous monitoring of the Live-Lab facility. The thermal and energy performance assessment was thus carried out in accordance with the requirements of the Croatian Technical regulation on energy economy and heat retention in buildings (Official Gazette No. 128/15 [38]).

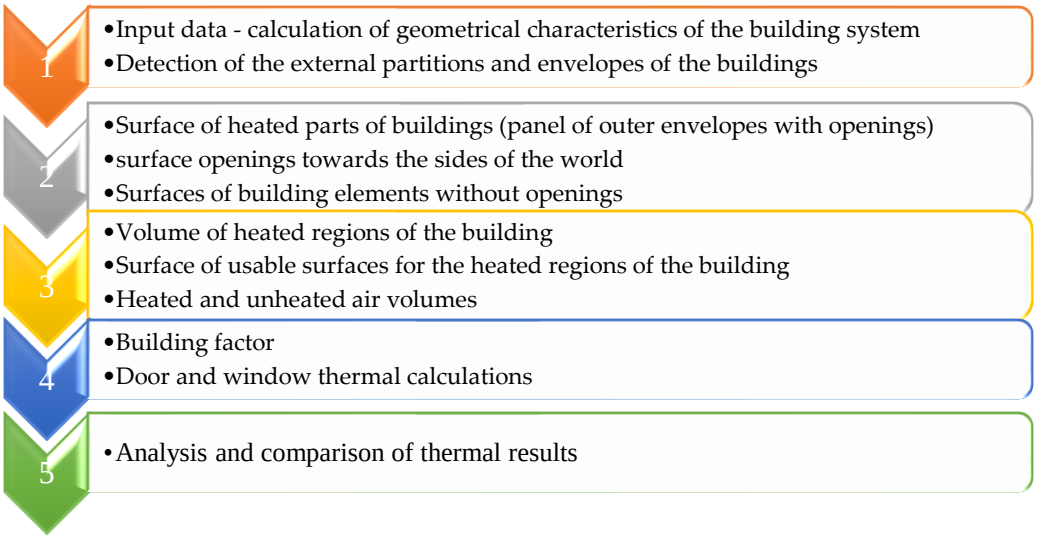


**Figure 8.** Schematic process for the thermal and energy analysis of the full-size facility.

Calculation of geometrical characteristics of the building envelope. As a basic step of the calculation process, the basic components of the envelope for the 3D facility were separately calculated, see Figure 9. This included two full-scale CLT-glass facade elements (East and West), and two solid walls (with a door opening for the Northside only).

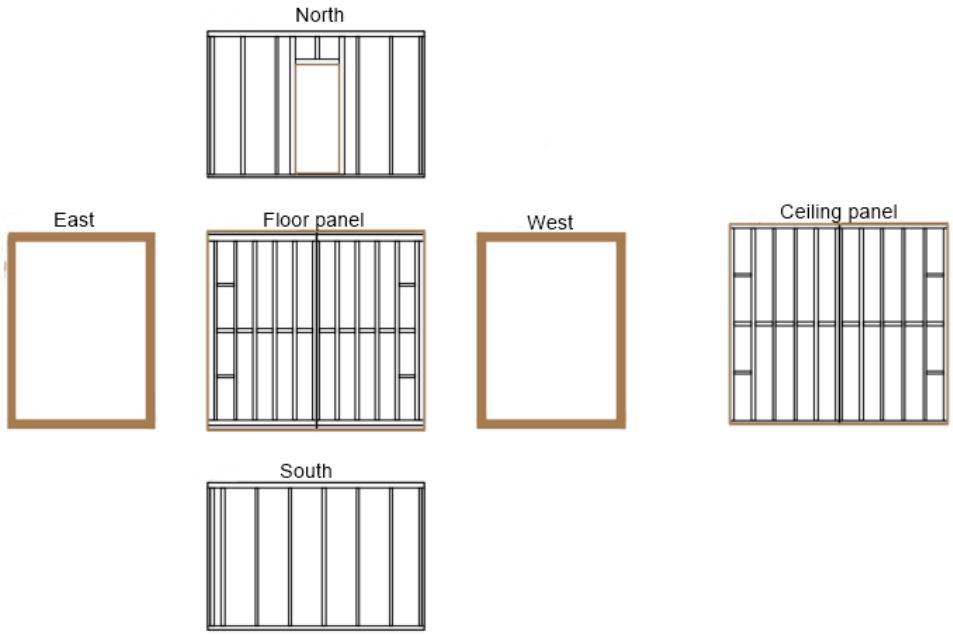


**Figure 9.** Arrangement of the envelope components for the full-size facility, as per cardinal directions.

Peer-reviewed version available at Appl. Sci. 2020, 10, 3071; doi:10.3390/app10093071



Afterward, the heated area for each cardinal direction was thus separately calculated, see Table 1. The same process was carried out to define the area for openings and openings on the heated boundaries - outside (Table 2).

**Table 1.** Building elements of the zone on the boundary heated - outside

| Exterior walls of the heated section with openings [m²] | | | |
|---|---|---|---|
| North | East | South | West |
| 10.98 | 9.82 | 10.98 | 9.82 |
| Heated exterior walls without openings [m²] | | | |
| North | East | South | West |
| 10.98 | 0.00 | 9.38 | 0.00 |

**Table 2.** Openings (number and size) of the facility, as per cardinal directions

| | Heated | | | Outside | | |
|---|---|---|---|---|---|---|
| Orientation | Opening mark | N.° of pieces | Width [m] | Height [m] | Surface [m²] | Total [m²] |
| East | P1 | 1 | 3.61 | 2.72 | 9.8192 | 9.8192 |
| North | Door | 1 | 0.8 | 2 | 1.6 | 1.6 |
| West | P1 | 1 | 3.61 | 2.72 | 9.8192 | 9.8192 |
| | The total area of openings | | | | | 21.24 |

The shape factor $f_0$ of the building - represented by the ratio of the surface to the volume of the heated part of the building – was finally defined, based on the heated area of the building ($A$=71.40 m²) and a reference volume of $V_e$= 46.49 m³:

$$f_0 = \frac{A}{V_e} = 1.54\ m^{-1} \quad (2)$$

*5.2. Calculation of windows and doors*

The 3D facility object of investigation is characterized by a large percentage of glass surfaces that are directly exposed to external environmental events. Accordingly, a large amount of gains (or losses) of energy is expected through such facade elements. It is thus of the utmost importance to prepare a detailed calculation of windows and doors, to obtain the best possible insight into the energy performance of the whole facility. The main parameters for windows and doors can be found in Tables 3-4.

**Table 3.** Double glazed window parameters.

| | | | |
|---|---|---|---|
| Heat transfer coefficient | $U_w$ | 2.42 | W/m²K |
| Degree of transmission of solar energy through glazing | $g^{\perp}$ | 0.64 | - |
| Window surface | $A_w$ | 9.82 | m² |
| Proportion of glazing | 1-$f_f$ | 0.8 | - |
| Panel | $f_p$ | 0 | - |
| Frame surface | $A_f$ | 1.964 | m² |

| | | | |
|---|---|---|---|
| Glazing surface | $A_g$ | 7.856 | m² |
| Panel surface | $A_p$ | 0 | m² |
| External glazing heat transfer coefficient | $U_{g1}$ | 5.15 | W/m²K |
| Degree of transmission of solar energy through glazing | $g^{\perp}{}_1$ | 0.80 | - |
| Internal glazing heat transfer coefficient | $U_{g2}$ | 5.15 | W/m²K |
| Degree of transmission of solar energy through glazing | $g^{\perp}{}_2$ | 0.80 | - |
| Thickness of the air cavity | $s$ | 35 | mm |
| Heat transfer coefficient of the frame | $U_f$ | 1.8 | W/m²K |
| Heat transfer coefficient of glass | $U_g$ | 2.51 | W/m²K |
| Heat transfer coefficient of the panel | $U_p$ | 0 | W/m²K |
| Glazing perimeter | $l_g$ | 11.54 | m |
| Linear thermal bridge (glass edge) | $\psi_g$ | 0.05 | W/mK |
| Panel perimeter | $l_p$ | 0 | m |
| Linear thermal bridge (panel edge) | $\psi_p$ | 0 | W/mK |
| Window inclination to horizontal | $\alpha$ | 90 | deg |
| Internal surface resistance | $R_{si}$ | 0.13 | m²K/W |
| External surface resistance | $R_{se}$ | 0.04 | m²K/W |
| $R_s$ | $R_s$ | 0.18 | m²K/W |

**Table 4**. Door parameters.

| | | | |
|---|---|---|---|
| Heat transfer coefficient | $U_w$ | 0.43 | W/m²K |
| Degree of transmission of solar energy through glazing | $g^{\perp}$ | 0.00 | - |

| | | | |
|---|---|---|---|
| Window surface | $A_w$ | 1.78 | m² |
| Proportion of glazing | 1-$f_f$ | 0.7 | - |
| Panel | $f_p$ | 0 | - |
| Frame surface | $A_f$ | 0.534 | m² |
| Glazing surface | $A_g$ | 1.246 | m² |
| Panel surface | $A_p$ | 0 | m² |
| Heat transfer coefficient of the external glazing | $U_f$ | 1 | W/m²K |
| Heat transfer coefficient of glass | $U_g$ | 0.18 | W/m²K |
| Degree of transmission of solar energy through glazing | $g^{\perp}$ | 0.00 | - |
| Heat transfer coefficient of the panel | $U_p$ | 0 | W/m²K |
| Glazing perimeter | $l_g$ | 0 | m |
| Linear thermal bridge (glass edge) | $\psi_g$ | 0.05 | W/mK |
| The perimeter of the panel | $l_p$ | 0 | m |
| Linear thermal bridge (panel edge) | $\psi_p$ | 0 | W/mK |
| Door inclination to horizontal | $\alpha$ | 90 | deg |

*5.3. Rational use of energy and thermal protection of the facility*

Preprints (www.preprints.org) | NOT PEER-REVIEWED | Posted: 23 March 2020 doi:10.20944/preprints202003.0330.v1

Peer-reviewed version available at Appl. Sci. 2020, 10, 3071; doi:10.3390/app10093071



Given that the facility is located at the Faculty of Civil Engineering of the University of Zagreb, the building category is defined in accordance with the Technical regulation on energy economy and heat retention in buildings [39, 40]. Accordingly, the latter can be intended as an independent building unit. The meteorological data obtained from the local station in the Live-Lab facility were taken into account for calculations, see Table 5.

**Table 5.** Meteorological data for Zagreb (from "Cycle 1" of Live-Lab measurements).

| | Month | | | | | | | | | | | |
|---|---|---|---|---|---|---|---|---|---|---|---|---|
| | Jan | Feb | Mar | Apr | May | Jun | Jul | Aug | Sep | Oct | Nov | Dec |
| Temperature $\Theta_e$ [°C] | 1.0 | 2.9 | 7.1 | 11.7 | 16.8 | 20.3 | 21.9 | 21.3 | 16.3 | 11.4 | 6.5 | 1.4 |
| Humidity $\varphi_e$ [%] | 81.0 | 74.0 | 68.0 | 67.0 | 66.0 | 67.0 | 67.0 | 69.0 | 76.0 | 80.0 | 83.0 | 85.0 |

The geometrical characteristics are presented below:

- volume of the heated part $V_e = 46.64$ m³
- net volume $V = 31.33$ m³
- net area $A_K = 11.52$ m²
- gross floor area $A_f = 14.95$ m²
- exterior surface area of heated part $A = 71.20$ m²
- shape factor $f_o = 1.54$ m$^{-1}$

Based on the recommendations of Technical Regulations, the overall impact of thermal bridges was taken into account by increasing the heat transfer coefficient of each part belonging to a heated section of the building, $U$ (W/m²K), with $U_{TM} = 0.05$ (W/m²K).

*5.4. Calculation of the building part*

Based on the parameters presented in Table 6, the heat transfer coefficient was calculated to verify that the requirement for dynamic thermal performance could be met, with respect to the reference limit value for the examined building (with $U_{max} = 0.30$ W/m²K).

**Table 6.** Building part: layout of the mineral wool panel and thermophysical properties (EN 13162 [41]).

| Layer | Material | Thickness $d$ | Specific heat capacity | Density $\rho$ | Thermal conductivity $\lambda$ | Differential resistance $S_d$ |
|---|---|---|---|---|---|---|
| 1 | 4.09 - directional chipboards (OSB) | 1.80 | 1700 | 650 | 0.130 | 0.9 |
| 2 | DELTA-DAWI-GP- vapour barrier | 0.02 | 1250 | 180 | 0.190 | 100 |
| 3 | 7.01 – mineral wool (MW) according to EN 13162 | 20.00 | 1030 | 30 | 0.040 | 0.2 |
| 4 | 4.09 - directional chipboards (OSB) | 1.80 | 1700 | 650 | 0.130 | 0.9 |
| | | 23.62 | | | | 102 |

For the case-study system herein presented, the heat transfer coefficient for the building part was obtained based on:

- the surface resistance, with $R_{si}$ = 0.13 m²K/W and $R_{se}$ = 0.04 m²K/W
- the thermal resistance of homogeneous layers, with:

$$R_T = R_{si} + \Sigma d_i/\lambda_i + R_{se} = 5.45 \text{ m}^2\text{K/W} \quad (3)$$

- and thus the heat transfer coefficient was finally calculated as:

$$U = 1/(R_T + R_u) + \Delta U = 0.18 \text{ W/m}^2\text{K} < 0.30 \text{ W/m}^2\text{K} \quad (4)$$

where $R_u$ is the thermal resistance of attic spaces (equal to 0).

It can be concluded the panel in use meets the minimum requirements for both heat transfer coefficient and dynamic thermal properties.

Surface condensation and internal condensation (Figure 10) greatly determine the comfort and usability of a given facility [42, 43]. They also define the conditions for mould occurrence. In Table 7, in this regard, the surface condensation and the distribution of the vapour pressure of water in the building part for the facility (low-intensity use mock-up) are proposed.

**Table 7.** Surface condensation risk assessment.

| Month | Vapour pressure in space $p_i$ [Pa] | Saturated vapour pressure $p_{sat}$ [Pa] | Surface temperature $\Theta_{si,min}$ [°C] | Temperature factor (Eq.(1)) $f_{Rsi}$ |
|---|---|---|---|---|
| Jan | 1.075 | 1.075 | 8.0 | 0.370 |
| Feb | 1.119 | 1.119 | 8.6 | 0.335 |
| Mar | 1.218 | 1.218 | 9.9 | 0.216 |
| Apr | 1.396 | 1.396 | 11.9 | 0.026 |
| May | 1.778 | 1.778 | 15.7 | - |
| Jun | 2.058 | 2.058 | 18.0 | - |
| Jul | 2.058 | 2.058 | 18.0 | - |
| Aug | 2.058 | 2.058 | 18.0 | - |
| Sep | 1.737 | 1.737 | 15.3 | - |
| Oct | 1.376 | 1.376 | 11.7 | 0.035 |
| Nov | 1.204 | 1.204 | 9.7 | 0.238 |
| Dec | 1.084 | 1.084 | 8.2 | 0.364 |

Preprints (www.preprints.org) | NOT PEER-REVIEWED | Posted: 23 March 2020 doi:10.20944/preprints202003.0330.v1

Peer-reviewed version available at Appl. Sci. 2020, 10, 3071; doi:10.3390/app10093071



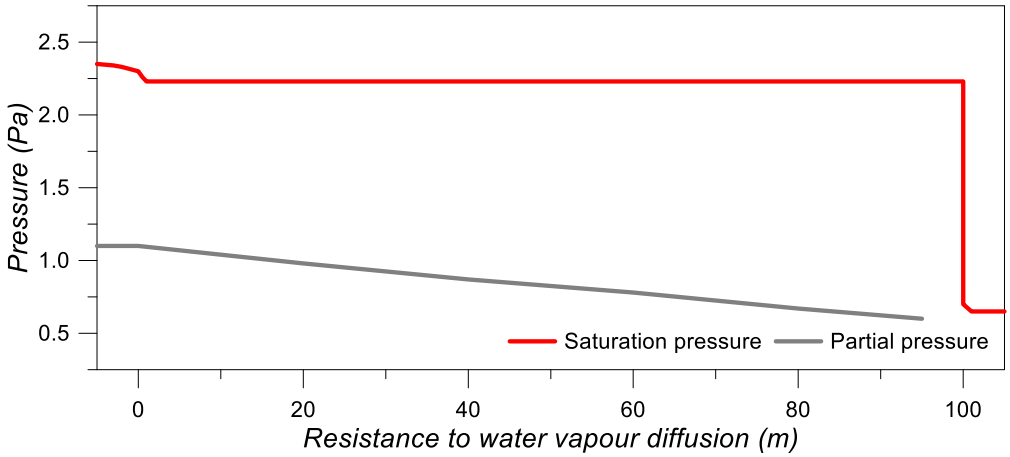


**Figure 10.** Internal condensation - Vapour pressure of water in the building part.

The building part, see Table 7, was found to meet the requirement for internal condensation. Given that the water vapour partial pressure curve in Figure 10 does not intersect the saturation pressure curve, it can be rationally concluded that the diffusion flow of water vapour through the wall is rather stationary, for the given climatic conditions.

On the other side, see Table 7, the calculate $f_{Rsi}$ values were found in a maximum of 0.37 that does not satisfy the minimum requirements recalled in Section 2. The latter can be justified in the simplified assumptions of the building numerical model and was thus further explored at the component level (see Section 6).

*5.5. Energy efficiency assessment*

Besides the simplified geometrical description of building details for the preliminary numerical model of the full-size prototype, some further considerations were derived in terms of energy efficiency that could be expected from the examined system. As such, Tables 8 and 9 show the distribution of heating and cooling energy required for the building facility, under the actual meteorological data. The direct heat losses through the transparent and non-transparent surfaces of the exterior envelopes, more in detail, are expressed by the transmission heat loss coefficient. Given that energy is partly lost through the soil and partly through the unheated spaces of the building, the heat losses were calculated with an increased thermal transmittance. The calculation process also included the coefficient of heat loss due to ventilation.

The energy required for cooling the facility, see Table 8, was found to reach the highest values from April to September, with $Q_C$ = 260 - 650 kWh. Similarly, see Table 9, the maximum energy required for heating are expected from November to February, with $Q_H$ = 300-460 kWh. The annual energy for heating and cooling was thus estimated in $Q_{H,nd}$ = 1.906 kWh/a and $Q_{c,nd}$ = 3.155 kWh/a respectively, with a relatively higher cooling energy consumption. High energy losses, however, are caused by thermal bridges due to different materials in use, as well as by linear thermal bridges due to geometry variations.

**Table 8.** Energy required for heating

Preprints (www.preprints.org) | NOT PEER-REVIEWED | Posted: 23 March 2020 doi:10.20944/preprints202003.0330.v1

Peer-reviewed version available at Appl. Sci. 2020, 10, 3071; doi:10.3390/app10093071



| Month | Outdoor temperature $\Theta e$ [°C] | Transmission losses $Q_{tr}$ [kWh] | Ventilation losses $Q_{ve}$ [kWh] | Overall losses $Q_{ls}$= [kWh] | Internal gains $Q_{int}$ [kWh] | Solar gains $Q_{sol}$ [kWh] | $Q_{gn}$ =$Q_{int}$+$Q_{sol}$ [kWh] | Losses/gains ratio $\gamma$=$Q_{gn}$/$Q_{ls}$ [-] | Used gains $\eta_{H,gn}$ [-] | Reduction factor $\alpha_{H,red}$ [-] | Required energy $Q_{nd,H}$ [kWh] |
|---|---|---|---|---|---|---|---|---|---|---|---|
| Jan | 1.0 | 933 | 88 | 1.021 | 43 | 218 | 261 | 0.26 | 0.886 | 0.58 | 461 |
| Feb | 2.9 | 759 | 72 | 831 | 39 | 342 | 381 | 0.46 | 0.787 | 0.58 | 310 |
| Mar | 7.1 | 643 | 60 | 703 | 43 | 598 | 641 | 0.91 | 0.611 | 0.58 | 182 |
| Apr | 11.7 | 411 | 37 | 448 | 41 | 802 | 843 | 1.88 | 0.401 | 0.58 | 65 |
| May | 16.8 | 176 | 15 | 191 | 43 | 996 | 1.039 | 5.44 | 0.170 | 0.58 | 9 |
| Jun | 20.3 | -1 | -1 | -3 | 41 | 1.030 | 1.071 | -389.46 | 0.000 | 1.00 | 0 |
| Jul | 21.9 | -87 | -9 | -95 | 43 | 1.094 | 1.137 | -11.92 | 0.000 | 1.00 | 0 |
| Aug | 21.3 | -58 | -6 | -65 | 43 | 962 | 1.005 | -15.57 | 0.000 | 1.00 | 0 |
| Sep | 16.3 | 188 | 17 | 204 | 41 | 744 | 785 | 3.84 | 0.230 | 0.58 | 14 |
| Oct | 11.4 | 440 | 40 | 479 | 43 | 508 | 551 | 1.15 | 0.544 | 0.58 | 105 |
| Nov | 6.5 | 657 | 61 | 717 | 41 | 244 | 285 | 0.40 | 0.815 | 0.58 | 283 |
| Dec | 1.4 | 919 | 86 | 1.006 | 43 | 158 | 201 | 0.20 | 0.915 | 0.58 | 479 |
| | | 4.979 | 459 | 5.438 | 505 | 7.696 | 8.201 | | | | 1.906 |

**Table 9.** The energy required for cooling

| Month | Outdoor temperature [°C] | Transmission losses [kWh] | Ventilation losses [kWh] | Overall losses [kWh] | Internal gains [kWh] | Solar gains [kWh] | $Q_{gn}$ =$Q_{int}$+$Q_{sol}$ [kWh] | Losses/gains ratio [-] | Used gains [-] | Reduction factor [-] | Required energy [kWh] |
|---|---|---|---|---|---|---|---|---|---|---|---|
| Jan | 1.0 | 1.035 | 97 | 1.132 | 43 | 218 | 261 | 0.23 | 0.899 | 0.58 | 15 |
| Feb | 2.9 | 852 | 80 | 932 | 39 | 342 | 381 | 0.41 | 0.810 | 0.58 | 42 |
| Mar | 7.1 | 745 | 69 | 815 | 43 | 598 | 641 | 0.79 | 0.653 | 0.58 | 130 |
| Apr | 11.7 | 510 | 46 | 556 | 41 | 802 | 843 | 1.52 | 0.462 | 0.58 | 265 |
| May | 16.8 | 278 | 24 | 302 | 43 | 996 | 1.039 | 3.44 | 0.253 | 0.58 | 453 |
| Jun | 20.3 | 98 | 8 | 105 | 41 | 1.030 | 1.071 | 10.18 | 0.095 | 0.58 | 566 |
| Jul | 21.9 | 16 | 0 | 16 | 43 | 1.094 | 1.137 | 70.14 | 0.014 | 0.58 | 654 |
| Aug | 21.3 | 44 | 3 | 47 | 43 | 962 | 1.005 | 21.36 | 0.046 | 0.58 | 559 |
| Sep | 16.3 | 287 | 26 | 312 | 41 | 744 | 785 | 2.51 | 0.324 | 0.58 | 310 |
| Oct | 11.4 | 542 | 49 | 591 | 43 | 508 | 551 | 0.93 | 0.605 | 0.58 | 127 |
| Nov | 6.5 | 756 | 70 | 825 | 41 | 244 | 285 | 0.35 | 0.841 | 0.58 | 27 |
| Dec | 1.4 | 1.022 | 96 | 1.117 | 43 | 158 | 201 | 0.18 | 0.926 | 0.58 | 9 |
| | | 6.183 | 569 | 6.752 | 505 | 7.696 | 8.201 | | | | 3.155 |

## 6. Thermal numerical analyses at the CLT-glass component level

### *6.1. Methods and assumptions*

A further attempt was carried out in the form of a thermal numerical analysis of the typical CLT-glass facade element in use for the Live-Lab system. The numerical investigation was carried out in ABAQUS [45]. Taking advantage of geometrical symmetry, the FE modelling was focused on

Preprints (www.preprints.org) | NOT PEER-REVIEWED | Posted: 23 March 2020 doi:10.20944/preprints202003.0330.v1

Peer-reviewed version available at Appl. Sci. 2020, 10, 3071; doi:10.3390/app10093071



¼ the nominal CLT-glass module of the Live-Lab mock-up. The use of symmetry restraints allowed then to enhance the computational cost of simulations.

The reference FE assembly, see Figure 11, consisted of a set of 8-node, heat transfer solid elements (DC3D8 type from ABAQUS library) representative of the nominal geometry for (i) the laminated glass sections (10.10/1.6); (ii) the interposed air cavity (s= 12.8mm); (iii) a rubber edge trim facilitating the glass panels to keep their position; (iv) the CLT frame members; (v) and the additional timber purlins providing a slot for the activation of frictional mechanisms along the edges of the glass.

The thermal performance of the CLT-glass facade module was hence assessed by evaluating few key performance indicators, such as the overall U-value, the corresponding -value (linear thermal transmittance) and the expected temperature scenario under the imposed gradient $T$ (for condensation risk assessment), with a focus on the minimum surface temperature on glass ($T_{min}$). The latter, according to Eq. (1), is directly responsible for the temperature factor at the internal surface $f_{Rsi}$ and thus overall thermal comfort.

The thermal boundary conditions for the FE steady-state simulations, based on EN ISO 10077-2:2017 [46] provisions, were defined as follows:

- Relative Humidity: 50%;
- External condition: $T$= 0°C, film coefficient (timber and glass)= 23 W/m²K;
- Internal condition: $T$= 20°C, film coefficient (timber and glass) = 8.02 W/m²K.

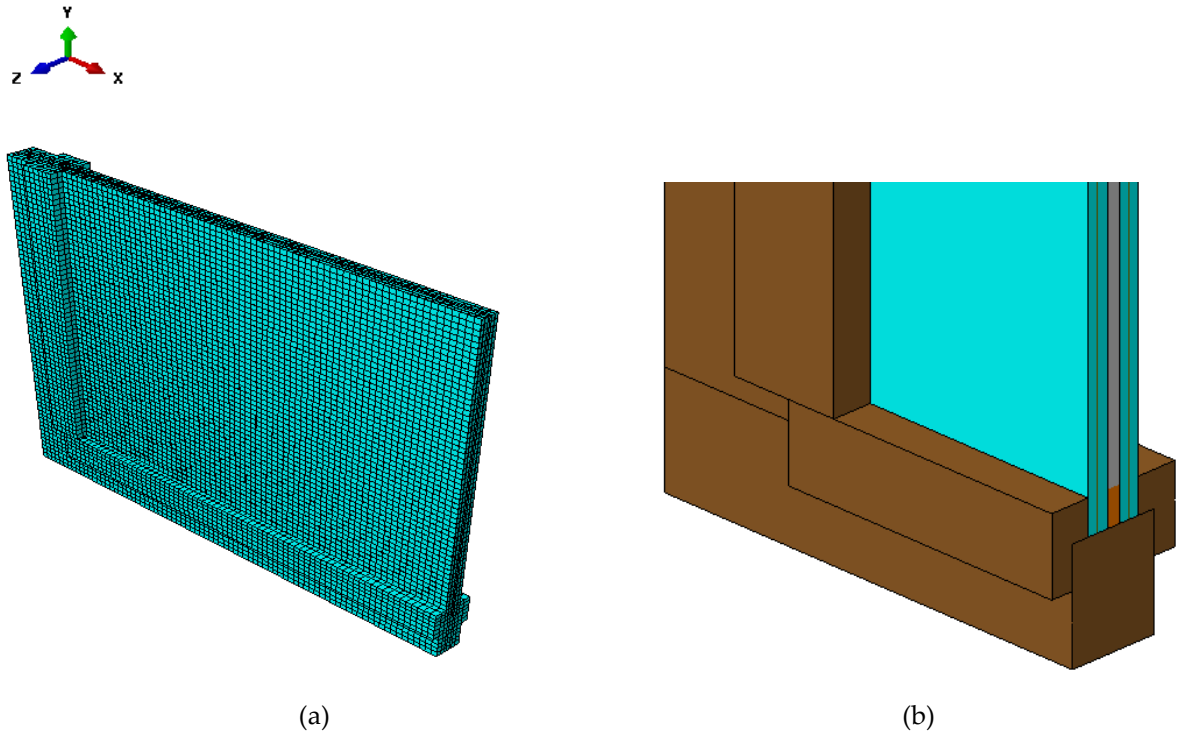


(a) (b)

**Figure 11.** Reference FE model for the thermal assessment of full-scale CLT-glass facade elements: (a) global assembly (1/4th the nominal geometry) and (b) detail view, with hidden mesh (ABAQUS)

The selected thermal scenario was found to be well representative of real field measurements available from the Live-Lab and average indoor conditions for a common building. For FE purposes, as in the case of transient analyses on small-scale prototypes, the thermal characterization of materials was carried out based on nominal thermo-physical parameters provided by design standards and literature references (Table 10).

**Table 10.** Input thermal properties in use for FE modelling in ABAQUS

| | Component | | | Interposed cavity | |
|---|---|---|---|---|---|
| | Glass | EVA | Timber | Rubber | Air |
| Conductivity $\lambda$ [W/mK] | 0.8 | 0.19 | 0.3 | 0.1 | 0.028 |
| Emissivity $\varepsilon$ [−] | 0.95 | / | 0.7 | / | / |

Special care was paid, in the latter case, for the air volume enclosed within the cavity between the laminated glass panels that was properly described in the form of conductivity. The latter assumes that the interposed cavity is perfectly sealed along the glass edges, and can be also extended to the VETROLIGNUM prototype (with frictional contacts with the timber frame, but a continuous flexible rubber to enclose the cavity).

The required *surface film* and *surface radiation* thermal interactions were defined on the internal and external surfaces of the outer glass panes and timber components, according to the boundary conditions earlier described. Along the longitudinal and transversal mid-section of the so assembled FE models, finally, symmetry conditions were accounted to reproduce the thermal performance of ¼ models as a part of the full-scale facade element.

### 6.2. *Some considerations on the expected thermal performance indicators*

The thermal assessment performance was carried out on the reference FE model, under an imposed thermal gradient of $\Delta T$= 20°C. Major FE outcomes are proposed in Table 11 in terms of U-total estimates, the corresponding $\Psi$-values and also max/min internal temperatures for glass ($T_{si,\,max}$ and $T_{si,\,min}$ respectively).

**Table 11.** Numerical thermal performance assessment of the CLT-glass component (ABAQUS).

| *Parameter* | Double laminated EVA (10.10/1.6)<br>*FE component model* |
|---|---|
| U-total [W/m²K] | 1.826 |
| $\psi$ -value | 0.5285 |
| Imposed $\Delta$T [°C] | 20 |
| $T_{si,max}$ [°C] | 16.60 |
| $T_{si,min}$ [°C] | 9.15 |

Besides, Figure 12 shows the typical temperature distribution in glass and a portion of timber frame members (corner region), for the reference CLT-glass system of Figure 11.

Preprints (www.preprints.org) | NOT PEER-REVIEWED | Posted: 23 March 2020 doi:10.20944/preprints202003.0330.v1

Peer-reviewed version available at Appl. Sci. 2020, 10, 3071; doi:10.3390/app10093071



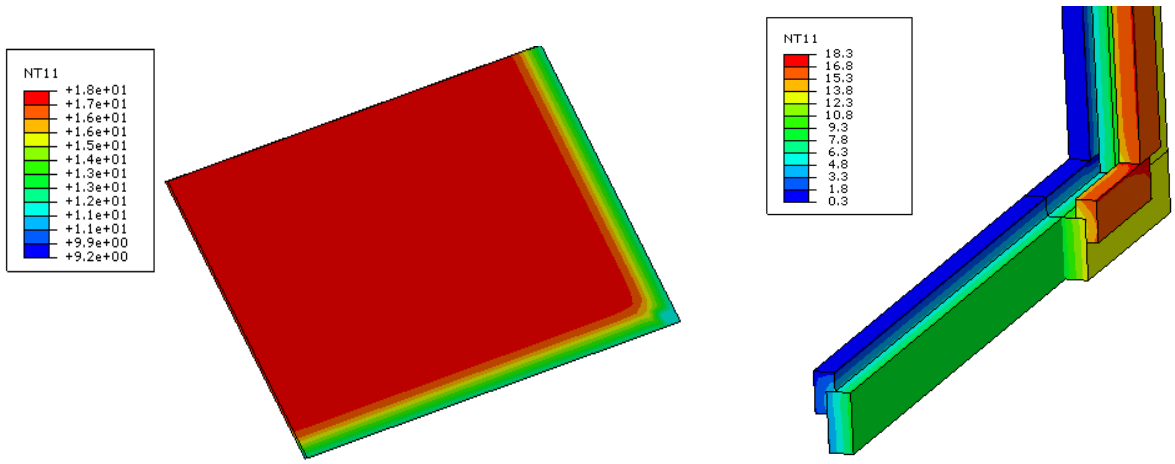


(a) (b)

**Figure 12.** FE thermal performance assessment of a full-scale CLT-glass facade element (ABAQUS). Expected distribution of temperature (a) in the internal glass panel (the external side) and (b) timber frame (values in °C).

Based on a more refined assessment of temperature distributions in timber and glass components, in Figure 12 it can be easily detected the region of glass in which contact with timber modifies its thermal response.

To this aim, Figure 13a shows the typical temperature distribution in the frame cross-section (CLT members and purlins), while Figure 13b offers a more detailed representation of temperatures in the thickness of glass.

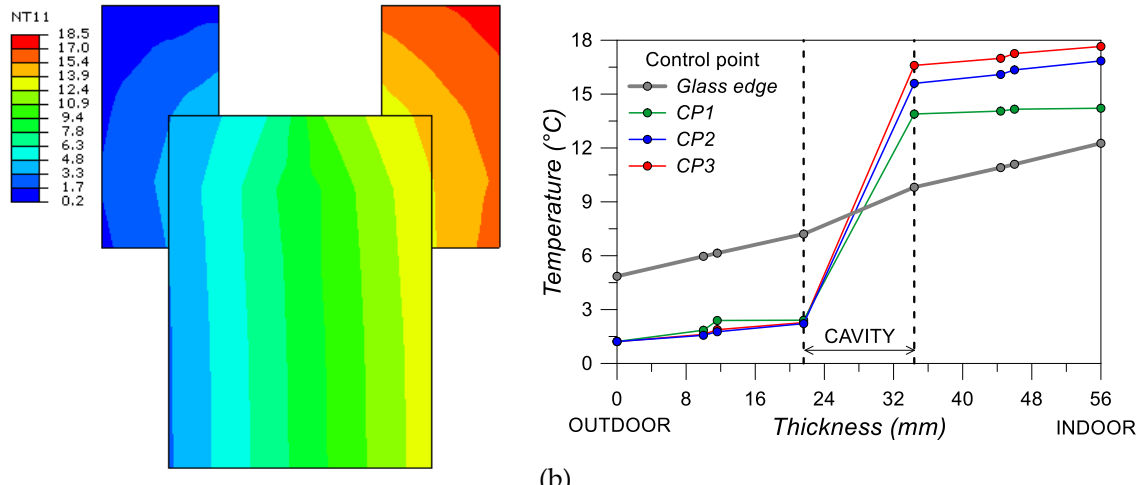


(a) (b)

**Figure 13.** FE thermal performance assessment of a full-scale CLT-glass facade element. Temperature distribution: (a) in the frame cross-section and (b) in the thickness of glass, with a focus on the corner region (ABAQUS, values in °C).

As far as the glass components are in contact with the frame of Figure 13a, the temperature distribution at the glass edges corresponds to the "Glass edge" plot in Figure 13b. In the same figure, the CP1, CP2 and CP3 control points are still representative of temperature distributions in the glass

thickness. According to the contour plot of Figure 12a, these CP$n$ values are selected on the diagonal of the glass panel, at a distance of 50mm, 90mm, and 150mm respectively from the corner.

To avoid condensation, as known, the minimum surface temperature ($T_{min}$) on the internal face of glass (i.e., inside the cavity volume) needs to be higher than the dew point temperature ($T_{dp}$) for air conditions occurring inside the panel, that is:

$$T_{min} \geq T_{dp} = f(RH, T) \quad (5)$$

The minimum measured surface temperature, for example, was calculated at 9.15°C (frame region), or higher. According to European standards, the reference $T_{dp}$ value for the examined boundary conditions should be checked based on mock up experiments including the continuous monitoring of temperature and humidity values inside the cavity. A similar approach was proposed also in [26] for a novel curtain wall system with a metal frame and represents a key design step for glass envelopes in general, especially concerning the detailing of framing members and sealants.

Conservatively, the calculation is carried out in this paper for the worst conditions in the cavity volume, which is an air temperature of 9°C and RH=80%. The corresponding $T_{dp}$ is estimated at 5.7°C, and consequently, the examined CLT-glass facade element (even in the critical regions of connection with the timber frame members) suggests an appropriate thermal performance. Its overall behaviour, however, will be further explored in the next stages of the project, with the support of the mock-up registrations.

Another relevant parameter is represented by the minimum surface temperature on the indoor face of the glass. In the latter case, for indoor conditions of 20°C and 50% of Relative Humidity, the recommended reference value is $T_{dp}$= 6°C, thus the limit condition is again optimally satisfied.

As far as the expected temperature factor $f_{Rsi}$ is taken into account and numerically calculated – at the component level – based on Eq.(1) during the winter season, the FE numerical system of Figure 11 finally results in:

$$f_{Rsi} = \frac{T_{si} - T_{out}}{T_{int} - T_{out}} = 0.613 \quad (6)$$

The so-calculate temperature factor is relatively higher, compared to the full-size preliminary numerical model of the mock-up building in Section 5. Besides, the latter is mostly in line with minimum requirements reported in Section 2, and further enforces the potentiality of the hybrid CLT-glass solution herein explored.

## 7. Discussion and conclusions

In this paper, an innovative hybrid structural element composed of Cross-Laminated timber (CLT) and laminated glass was analyzed. The beginning of the development for the design concept for this element dates 2006, when it was conducted within the Ministry of Education and Science of Republic of Croatia financed projects “Composite structural systems timber-structural glass and timber-steel” (coordinator prof. Vlatka Rajčić), after that within bilateral project 2010- 2012 Croatia-North Macedonia, coordinators prof. Vlatka Rajčić and prof. Lidija Krstevska “Seismic resistance of composite timber-structural glass structural systems with the optimal level of energy dissipation”. Further developments continued within the project funded by the Croatian Science Foundation “VETROLIGNUM - Multipurpose structural panel”.

Differing from conventional solutions for facades, the design concept is based on the avoidance of stress concentrations at the CLT and laminated glass joints, due to the use of mechanical fasteners or adhesives. The joint is designed as a contact joint over friction surfaces. The hybrid element has shown excellent performance at static, dynamic and earthquake loads. It is designed to have good structural performance. As the most intended purpose of applying these large panels as facade elements, however, several other characteristics and performance parameters must be addressed and possibly optimized (i.e., energy efficiency, water-tightness, airtightness, optimal thermal characteristics, durability, required lightening comfort, etc.).

The focus of this paper, accordingly, was to evaluate under ordinary operational conditions the thermal performance of the hybrid panel prototype which is non optimised in the sense of high energy performances,. The expected thermal performance was analyzed based on the behaviour of the hybrid panel under climate configurations for the Croatian region, by using records from a Live-Lab mock-up building that is currently installed at the University of Zagreb. The ambient records were used to numerically assess the thermal and energy performance indicators for a full-size building prototype, as well as to further assess the component detail behaviours.

From the full-size numerical model, for example, the same boundary conditions of the built-in Live-Lab were taken into account, thus focusing on the calculation of a few key thermal and energy parameters. Besides the use of simplified numerical approaches, the building analysis pointed out the critical regions that should be further optimized for enhanced thermal responses, due to the presence of thermal bridges. They were found to be primarily located in the corner regions of the CLT frame members, as well as in the CLT-to-glass contacts between the various building components. In addition to the continuous monitoring of external climatic parameters, indoor conditions thermal parameters of facade element, a more refined Finite Element model was also developed to locally evaluate the typical thermal response of a CLT-glass facade component. The numerical model, as shown, proved a rather sufficient energy performance for the hybrid panel, according to European as well as national requirements.

In the next stages of the research, the priority of investigations will be oriented towards the improvement of the design details in the region of contact between different building components and materials, as well as to explore new sealing products and various options for adaptive solutions (shading systems, etc.).

**Author Contributions:**

Conceptualization, Vlatka Rajčić and Chiara Bedon; Data curation, Nikola Perković, Chiara Bedon and Jure Barbalić; Formal analysis, Nikola Perković and Chiara Bedon; Funding acquisition, Vlatka Rajčić; Investigation, Vlatka Rajčić, Nikola Perković and Jure Barbalić; Methodology, Vlatka Rajčić and Chiara Bedon; Project administration, Vlatka Rajčić, Nikola Perković and Jure Barbalić; Resources, Vlatka Rajčić; Software, Nikola Perković and Chiara Bedon; Supervision, Vlatka Rajčić, Chiara Bedon and Roko Zarnic; Validation, Vlatka Rajčić, Nikola Perković, Chiara Bedon, Jure Barbalić and Roko Zarnic; Visualization, Chiara Bedon and Roko Zarnic; Writing – original draft, Vlatka Rajčić, Nikola Perković and Chiara Bedon.

**Funding:** This research was funded by The Croatian Science Foundation (Project no. IP-2016-06-3811 VETROLIGNUM – “Prototype of multipurpose composite timber-load bearing glass panel”, coordinator Prof. Vlatka Rajčić, University of Zagreb, Croatia).

**Conflicts of Interest:** The authors declare no conflicts of interest. The funders had no role in the design of the study; in the collection, analyses, or interpretation of data; in the writing of the manuscript, or in the decision to publish the results.

## References

1. Cruz, P., Pequeno, J. (2008). Timber-glass composite beams: Mechanical behaviour & architectural solutions. Challenging Glass Proceedings, pp. 439-448
2. Premrov, M., Zlatinek, M., Štrukelj, A. (2014). Experimental analysis of load-bearing timber-glass I-beam. Constr Unique Build Struct, 4(19): 11-20
3. Rodacki, K., Tekieli, M., Furtak, K. (2019). Contactless optical measurement methods for glass beams and composite timber-glass I-beams. Measurement, 134: 662-672
4. Blyberg, L., Lang, M., Lundstedt, K., Schander, M., Serrano, E., Silfverhielm, M., Stälhandske, C. (2014). Glass, timber and adhesive joints - innovative load bearing building components. Construction and Building Materials, 55: 470-478
5. Neubauer, G. (2011). Entwicklung und Bemessung von statisch wirksamen Holz-Glas-Verbundkonstruktionen zum Einsatz im Fassadenbereich [Development and dimensioning of structurally effective wood-glass composites for use in the facade sector (in German)]. Ph.D. Thesis, University of Technology TU Wien, *http://repositum.tuwien.ac.at/obvutwhs/content/titleinfo/1614407*
6. Ber, B., Premrov, M., Sustersic, I., Dujic, B. (2013). Innovative earthquake resistant timber-glass buildings. Natural Science, 5: 63-71. doi: 10.4236/ns.2013.58A1008
7. Antolinc, D. (2013). Uporaba steklenih panelov za potresno varno gradnjo objektov [Use of laminated glass panels for earthquake resistant building design (in Slovenian)]. Ph.D. Thesis, University of Ljubljana, *http://drugg.fgg.uni-lj.si/4588/*
8. Rajčić, V., Žarnić, R (2012). Seismic response of timber frames with laminated glass infill. CIB-W18/45-15-4, pp. 333-344, Växjo, Sweden
9. Žarnić, R., Rajčić, V., Kržan, M. (2020). Response of laminated glass-CLT structural components to reverse-cyclic lateral loading. Construction and Building Materials, 235: 117509
10. Jeleč, M., Varevac, D., Rajčić, V. (2018). Križno lamelirano drvo (CLT) - pregled stanja područja [Cross Laminated Timber (CLT) – A state of the art report], Građevinar, 70(2): 75-95 (Journal of the Croatian Association of Civil Engineers)
11. Bejtka, I. (2011). Cross (CLT) and diagonal (DLT) laminated timber as innovative material for beam elements. Karlsruhe, KIT Scientific Publishing
12. EN 12543-2. Glass in building - Laminated glass and laminated safety glass - Part 2: Laminated safety glass. CEN - European Committee for Standardization, Brussels, Belgium
13. prEN 13474-2 Glass in building - Design of glass panes – Part 2: Design for uniformly distributed loads. CEN - European Committee for Standardization, Brussels, Belgium
14. Feldmann, M., Di Biase, P. (2018). The CEN-TS "Structural Glass – Design and Construction Rules" as pre-standard for the Eurocode. ce/papers, 2(5-6): 71-80. Special Issue: Engineered Transparency 2018 – Glass in Architectural and Structural Engineering, doi: 10.1002/cepa.911
15. CEN/TC 250 (2019). prCEN/TS xxxx-1: 2019 - In-plane loaded glass components (December 2019). CEN - European Committee for Standardization, Brussels, Belgium

16. CEN/TC 250 (2019). prCEN/TS xxxx-2:2019 - Out of-plane loaded glass components (December 2019). CEN - European Committee for Standardization, Brussels, Belgium
17. CNR-DT 210/2013 (2013). Istruzioni per la Progettazione. l'Esecuzione ed il Controllo di costruzioni con Elementi Strutturali in Vetro [Guideline for design, execution and control of constructions made of structural glass elements (in Italian)]. National Research Council (CNR), Roma, Italy, *www.cnr.it*
18. Buildings Department (2018). Code of practice for the structural use of glass (*http://www.bd.gov.hk./*)
19. Feldmann, M., Kasper, R., et al. (2014). Guidance for European structural design of glass components – support to the implementation, harmonization and further development of the Eurocodes. Dimova, Feldmann Pinto, Denton (Eds.), Report EUR 26439–Joint Research Centre-Institute for the Protection and Security of the Citizen, doi: 10.2788/5523
20. Bedon, C. (2017). Structural glass systems under fire: Overview of design issues, experimental research and developments. Adv. Civil Eng., 2017, doi: 10.1155/2017/2120570
21. Sjöström, J., Kozlowski, M., Honfi, D., Lange, D., Albrektsson, J., Lenk, P., Eriksson, J. (2020). Fire Resistance Testing of a Timber-Glass Composite Beam. International Journal of Structural Glass and Advanced Materials Research (accepted for publication, 17 pages, proof available online: *https://thescipub.com/abstract/10.3844/ofsp.12922*)
22. Bedon, C., Louter, C. (2018). Thermo-mechanical numerical modelling of structural glass under fire - Preliminary considerations and comparisons. Proceedings of Challenging Glass - International Conference on Architectural and Structural Applications of Glass, May 11-13, Delft University, Belgium, pp: 513-524, doi: 10.7480/cgc.6.2173
23. Kozlowski, M., Bedon, C., Honfi, D. (2018). Numerical Analysis and 1D/2D Sensitivity Study for Monolithic and Laminated Structural Glass Elements under Thermal Exposure. Materials, 11(8), 1447, doi.: 10.3390/ma11081447
24. EN 1995-1-1: 2004. Eurocode 5: Design of timber structures - Part 1-1: General - Common rules and rules for buildings. CEN - European Committee for Standardization, Brussels, Belgium
25. EU 2010/31. European Commission – Directive 2010/31/EU of the European Parliament and of the Council, *https://eur-lex.europa.eu/legal-content/EN/TXT/HTML/?uri=CELEX:32010L0031&from=HR*
26. Zobec, M., Colombari, M., Peron, F., Romagnoni, P. (2002). Hot-box tests for building envelope condensation assessment. Proceedings of 23rd AIVC and EPIC 2002 Conference (in conjunction with 3rd European Conference on Energy Performance and Indoor Climate in Buildings) - Energy efficient and healthy buildings in sustainable cities, Lyon, France
27. Aldawoud, A. (2017). Assessing the energy performance of modern glass facade systems. MATEC Web of Conferences, 120: 08001, doi: 10.1051/matecconf/201712008001
28. Bedon, C., Pascual, C., Navarro, A.L., Overend, M. (2018). Thermo-mechanical Investigation of Novel GFRP-glass Sandwich Facade Components. Challenging Glass Proceedings, vol. 6: 501-512, doi: 10.7480/cgc.6.2172
29. Planas, C., Cuerva, E., Alavedra, P. (2018). Effects of the type of façade on the energy performance of office buildings representative of the city of Barcelona. Ains Shams Engineering Journal, 9(4): 3325-3334
30. Pelaz, B., Blanco, J.M., Cuadrado, J., Egiluz, Z., Buruaga, A. (2017). Analysis of the influence of wood cladding on the thermal behavior of building façades; characterization through simulation by using different tools and comparative testing validation. Energy and Buildings, 141: 394-360

31. Favoino, F., Loonen, R.C.G.M., Doya, M., Goia, F., Bedon, C., Babich, F. (2018). Building Performance Simulation and Characterisation of Adaptive Facades – Adaptive Facade Network. ISBN 978-94-6366-111-9, published by TU Delft Open for the COST Action 1403 Adaptive Facade Network
32. EN ISO 13788. Hygrothermal performance of building components and building elements – Internal surface temperature to avoid critical surface humidity and interstitial condensation – Calculation methods. International Organization for Standardization (ISO), Brussels, Belgium
33. Kalamee, T. (2006). Critical values for the temperature factor to assess thermal bridges. Proc. Estonian Acad. Sci. Eng., 12(3-1): 218–229
34. Zanor, D., Pretty, J., Morrison, J., Todorovic, S.K. (2005). Environmental and macroeconomic impact assessment of different development scenarios to organic and low-input farming in Croatia. Technical Report, ID 26404, University of Essex, Colchester. Free download at: *http://www.fao.org/docs/eims/upload/229899/2005_12_doc02.pdf*
35. EN 338: 2016. Structural timber - Strength classes. European Committee for Standardization (CEN), Brussels, Belgium
36. KNAUF Insulation® technical data sheet (*www.knaufinsulation.hr/proizvodi-0/naturboard-venti*)
37. DELTA® technical data sheet (*https://www.doerken.com/int/products/pitched-roof/delta-dawi-gp.php*)
38. Ordinance on energy audits and energy certification of buildings OG (88/17), Technical regulation on energy economy and heat retention in buildings OG 128/15, Technical regulation for windows and doors OG 69/06
39. EN 12524: 2002. Building materials and products - Hygrothermal properties - Tabulated Design Values. CEN - European Committee for Standardization, Brussels, Belgium
40. EN ISO 13790: 2008 Energy performance of buildings - Calculation of energy use for space heating and cooling. CEN - European Committee for Standardization, Brussels, Belgium
41. EN 15251: 2008 Indoor environmental input parameters for design and assessment of energy performance of buildings addressing indoor air quality, thermal environment, lighting and acoustics. CEN - European Committee for Standardization, Brussels, Belgium
42. EN 13162 : 2012 + A1: 2015. Thermal insulation products for buildings. Factory made mineral wool (MW) products. Specification. CEN - European Committee for Standardization, Brussels, Belgium
43. Republic of Croatia, Ministry of Construction and Urban Planning (2013). Building Act, Official Gazette 153/13, 20/17 (*https://mgipu.gov.hr/access-to-information/regulations-126/regulations-in-the-field-of-building-127/127*)
44. Republic of Croatia, Ministry of Construction and Urban Planning (2014). Energy Efficiency Act, Official Gazette 127/14, 116/18 (*https://mgipu.gov.hr*)
45. Simulia (2019). ABAQUS v.6.14 computer software and online documentation, Dassault Systems, Providence, RI, USA
46. EN ISO 10077-2. Thermal performance of windows, doors and shutters - Calculation of thermal transmittance - Numerical methods for frames. CEN - European Committee for Standardization, Brussels, Belgium